Applied Physics Letters ARTICLE pubs.aip.org/aip/apl

# Direct evidence and thermodynamics for the conversion between nitrogen pairs and interstitial nitrogen atoms in nitrogen-doped Czochralski silicon

Cite as: Appl. Phys. Lett. **126**, 142106 (2025); doi: 10.1063/5.0252869
Submitted: 12 December 2024 · Accepted: 27 March 2025 ·
Published Online: 7 April 2025



Tong Zhao,[1,2] Defan Wu,[1] Qunlin Nie,[1] Hao Chen,[1] Xiangyang Ma,[1,2,a)] and Deren Yang[1,2,a)]

## AFFILIATIONS

[1]State Key Laboratory of Silicon and Advanced Semiconductor Materials and School of Materials Science and Engineering, Zhejiang University, Hangzhou 310027, China
[2]Shangyu Institute of Semiconductor Materials, Shaoxing 312300, Zhejiang Province, China

[a)]**Authors to whom correspondence should be addressed:** mxyoung@zju.edu.cn and mseyang@zju.edu.cn

## ABSTRACT

The conversion between di-interstitial nitrogen ($N_2$) pairs and interstitial nitrogen ($N_i$) atoms has long been conceptually presented to understand the nitrogen behaviors in nitrogen-doped Czochralski (NCZ) silicon, unfortunately, lacking direct experimental evidence. In this work, we report on the experimental findings that demonstrate the remarkable dissociation of $N_2$ pairs into $N_i$ atoms in NCZ silicon quenched from an isothermal anneal at a high temperature in the range of 1050–1250 °C. Moreover, it is found that the $N_i$ atoms dissociated from the $N_2$ pairs at a high temperature can revert to the $N_2$ pairs at a lower temperature. The aforementioned results have been well understood in terms of thermodynamic analysis and molecular dynamics simulations. We believe that this work gives an insight into the defect engineering in CZ silicon by means of nitrogen-doping.





Nitrogen-doping in Czochralski (CZ) silicon has been recognized as an effective approach to improving the mechanical strength, enhancing the capability of internal gettering associated with oxygen precipitation and facilitating the annihilation of voids.[1–11] Consequently, nitrogen-doped CZ (NCZ) silicon has been widely applied in manufacturing integrated circuits. In either CZ or float-zone silicon, the nitrogen impurities are usually found to exist predominantly in the form of di-interstitial nitrogen ($N_2$) pairs at room temperature (RT), which can be manifested by 963 $cm^{-1}$ absorption peak in a Fourier transformation infrared (FTIR) spectrum.[12–16] However, whether or not the nitrogen impurities doped in the molten silicon are directly converted into the $N_2$ pairs in the grown silicon crystal is yet to be answered. For NCZ silicon, the nitrogen impurities can interact with the oxygen impurities to form extended defects under certain conditions. It has been found that annealing NCZ silicon at relatively low temperatures (e.g., 350–650 °C) leads to generating a series of nitrogen-oxygen (N-O) complexes featuring shallow thermal donors, thus, denoted as N-O STDs.[17–23] Based on the experimental finding that the concentration of N-O STDs is proportional to the square root of nitrogen concentration, Voronkov *et al.* proposed that only one interstitial nitrogen ($N_i$) atom, dissociated from a $N_2$ pair, was involved in the formation of a N-O STD.[24] Moreover, an atomistic model was proposed for nitrogen diffusion in silicon, wherein the nitrogen impurities diffused via the $N_i$ atoms dissociated from the $N_2$ pairs at high temperatures.[25–29] In contrast, other researchers deduced that the nitrogen diffusion in silicon was dominantly via the $N_2$ pairs even at the temperatures up to 1200 °C.[30–34] The aforementioned dispute in the community is due to that there is no unequivocal experimental evidence for both the existence of $N_i$ atoms and the conversion between the $N_2$ pairs and $N_i$ atoms in silicon.

Although the theoretical calculations have predicted that the $N_i$ atoms in silicon can be manifested by the infrared absorption peak at ~550 $cm^{-1}$,[16,35] the related experimental evidence has not been reported so far. This could be attributed to either the absence of $N_i$ atoms or the concentration of the $N_i$ atoms retained at RT being lower than the detection limit of FTIR spectroscopy. However, from the thermodynamic point of view, we believe that the conversion between the $N_2$ pairs and $N_i$ atoms is possible. Intuitively, at a sufficiently high

temperature, the $N_2$ pairs may be dissociated into the $N_i$ atoms due to the violent thermal vibrations. Therefore, the challenge for the detection of $N_i$ atoms is how to retain as many $N_i$ atoms dissociated from the $N_2$ pairs as possible. To address such a challenge, in this work, we present a dedicated quenching method for the NCZ silicon annealed at elevated temperatures. As a result, the existence of $N_i$ atoms and the conversion between the $N_2$ pairs and $N_i$ atoms in the quenched NCZ silicon are unveiled by FTIR spectroscopy at RT. Moreover, the achieved experimental results have been essentially understood in terms of thermodynamic analysis and molecular dynamics (MD) simulations.

One ⟨100⟩-oriented, 2.5 mm thick, 150 mm-diameter, *n*-type NCZ silicon wafer with a resistivity of 16.8 Ω cm was used. In such a wafer, the nitrogen concentration was $2.5 \times 10^{15}\,cm^{-3}$, measured by secondary ion mass spectroscopy (SIMS). The interstitial oxygen concentration ($[O_i]$) was determined to be $7.60 \times 10^{17}\,cm^{-3}$ by FTIR spectroscopy, with a calibration coefficient of $3.14 \times 10^{17}\,cm^{-2}$. A few of the specimens, with a size of $1.5 \times 1.5\,cm^2$, were cleaved from the aforementioned wafer for different isothermal anneals at temperatures ranging from 900 to 1250 °C for 5 min in an argon ambient, carried out in a quartz tube furnace. In this work, two cooling methods were adopted after the isothermal anneals. One was quenching, for which the annealed specimens were directly withdrawn into trimethylsilanol with a volume of 3 L, followed with the successive cleaning in acetone and de-ionized water. The other was air-cooling, for which the annealed specimens were withdrawn into the air. Each annealed specimen was subjected to the double-sided chemical mechanical polishing to substantially remove the nitrogen out-diffusion zones formed by the isothermal anneal at an elevated temperature, resulting in a final thickness of 2 mm. The specimens quenched or air-cooled from the aforementioned isothermal anneals were characterized by FTIR at RT. Herein, it should be mentioned that the FTIR spectrum of each investigated NCZ silicon specimen was obtained by subtracting that of the CZ control, whose $[O_i]$ and thickness were almost the same as those of the NCZ silicon specimen. Moreover, the CZ control received the same anneal of the investigated NCZ silicon specimen. In addition, the quenched and air-cooled specimens with the 1200 °C/5 min anneal were subjected to the subsequent isothermal anneal at 650 °C carried out in an argon ambient for the formation of N-O STDs. The concentration of N-O STDs was derived from the difference between the carrier concentrations before and after the 650 °C anneal. Herein, the carrier concentrations were transformed from the resistivities measured by four-point probe (FPP) according to the ASTMF723-88 standard.

The static density functional theory (DFT) calculations and MD simulations were carried out using the Vienna *Ab initio* Simulation Package (VASP). The Perdew–Burke–Ernzerhof (PBE) exchange-correlation functional at the generalized gradient approximation (GGA) level was adopted.[36,37] For the static DFT calculations, a silicon supercell consisting of 216 Si atoms and a $N_2$ pair aligned along ⟨110⟩ orientation was constructed, followed with the geometric optimization. To this end, a $2 \times 2 \times 2$ *k*-point sampling of the Brillouin zone and a plane wave basis set with a cutoff energy of 450 eV were employed. The structure was optimized until the force on each atom was less than 0.01 eV/Å, with an energy convergence threshold of $1.0 \times 10^{-5}$ eV. MD simulations were performed on the optimized supercell to learn the thermal stability of $N_2$ pair. To this end, the NVT ensemble was applied, and the temperature of supercell was set as 900, 1050, 1150, 1200, or 1350 °C. The MD simulations employed a step time of 1 fs for 1000 steps, with an energy convergence criterion set to be $5.0 \times 10^{-5}$ eV.

The upper panel of Fig. 1(a) shows the mid-infrared FTIR spectra for the NCZ silicon specimens subjected to the 1200 °C/5 min anneal with the quenching and air-cooling methods, respectively, as well as a reference spectrum of the as-received NCZ silicon specimen with a thickness of 2 mm. It is well documented that the IR absorption peaks at 963 and 541 $cm^{-1}$ correspond to the $N_2$ pairs and $N_i$ atoms in silicon, respectively.[13,35] As can be seen from Fig. 1(a), the concentration of $N_i$ atoms is highest in the quenched specimen, while that is negligible in the as-received specimen. Moreover, the air-cooled specimen shows an intermediate $N_i$ concentration. Noteworthily, the intensity of 541 $cm^{-1}$ peak increases along with the decrease in the intensity of the 963 $cm^{-1}$ peak, suggesting that the $N_i$ atoms are converted from the $N_2$ pairs. Figure 1(b) shows the changes in N-O STD concentrations in the two NCZ silicon specimens subjected to the 650 °C anneal for different times, following the 1200 °C/5 min anneal with the quenching and air-cooling methods, respectively. Evidently, the quenched specimen exhibits a substantially higher generation rate of N-O STDs than the air-cooled specimen in the early stage of 650 °C anneal. Voronkov *et al.* verified the involvement of only one $N_i$ atom and several ($x$) $O_i$ atoms, about three on average, in a N-O STD produced at 650 °C.[24] Therefore, the formation of N-O STDs can be expressed as

$$N_i + xO_i \leftrightarrow NO_x. \quad (1)$$

According to the law of mass action, the generation rate of N-O STDs is directly proportional to the concentration of $N_i$ atoms. As seen in Fig. 1(b), the quenched specimen exhibits a substantially higher generation rate of N-O STDs than the air-cooled specimen at the early stage of 650 °C anneal. Thus, it can be deduced that the quenched specimen contains much more $N_i$ atoms than the air-cooled counterpart, which is consistent with the result revealed in the upper panel of Fig. 1(a). The lower panel of Fig. 1(a) shows the mid-infrared FTIR spectrum for the NCZ silicon subjected to the 900 °C/5 min anneal after the quenching from the 1200 °C/5 min anneal. Comparing this FTIR spectrum with that of the quenched specimen, shown as the bottom one in the upper panel of Fig. 1(a), it is found that the intensity of 541 $cm^{-1}$ peak decreases remarkably, while that of 963 $cm^{-1}$ peak increases a little due to the additional 900 °C/5 min anneal. This indicates that a number of $N_i$ atoms in the quenched specimen revert to the $N_2$ pairs during the additional 900 °C/5 min anneal. Therefore, it is verified that the $N_i$ atoms are not thermodynamically stable at a lower temperature so that they are inclined to convert into the $N_2$ pairs. In brief, the conversion between the $N_2$ pairs and $N_i$ atoms, which was just a conceptual picture previously, has been experimentally evidenced as shown in Fig. 1.

Figure 2(a) illustrates a series of middle-infrared FTIR spectra for the NCZ silicon specimens quenched from the isothermal anneals at different temperatures ranging from 900 to 1250 °C for 5 min. For comparison, the FTIR spectrum of the as-received NCZ silicon specimen is also included. It is evident that the intensity of 541 $cm^{-1}$ peak ($I_{541}$) changes remarkably with the annealing temperature, while that of 963 $cm^{-1}$ peak ($I_{963}$) shows relatively minor variations. For clarity, Fig. 2(b) shows the ratio of $I_{541}$ to $I_{963}$ ($I_{541}/I_{963}$) for each specimen in Fig. 2(a). As can be seen, at the temperatures no more than 950 °C, the

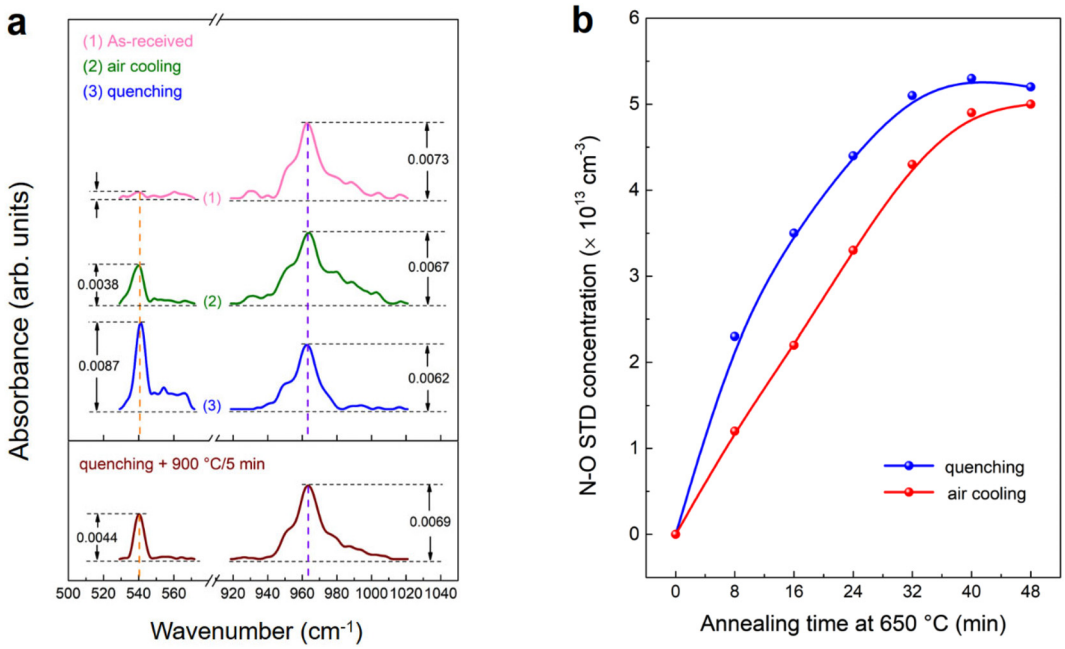


**FIG. 1.** (a) In the upper panel: the mid-infrared FTIR spectra for the NCZ silicon specimens subjected to the 1200 °C/5 min anneal with the quenching and air-cooling methods, respectively, together with a reference spectrum of the as-received specimen. In the lower panel: the mid-infrared FTIR spectrum for the NCZ silicon specimen subjected to the 900 °C/5 min anneal after the quenching from the 1200 °C/5 min anneal. (b) The changes in N-O STD concentrations in the two NCZ silicon specimens subjected to the 650 °C anneal for different times, following the 1200 °C/5 min anneal with the quenching and air-cooling methods, respectively.

ratio of $I_{541}/I_{963}$ is negligible, suggesting that the nitrogen impurities in silicon predominantly exist in the form of $N_2$ pairs. When the annealing temperature exceeds 950 °C, the ratio of $I_{541}/I_{963}$ increases significantly with the increasing temperature, indicating that the increase in temperature favors the dissociation of $N_2$ pairs into $N_i$ atoms. The temperature-dependent conversion between the $N_2$ pairs and $N_i$ atoms can be essentially understood by the following thermodynamic analysis.

The conversion between the $N_2$ pairs and $N_i$ atoms can be expressed as

$$N_2 \overset{k}{\longleftrightarrow} 2N_i, \tag{2}$$

where $k$ is the equilibrium constant of the forward reaction, namely, the dissociation of $N_2$ pairs into $N_i$ atoms, in Eq. (2), which can be derived from

$$k = \frac{[N_i]^2}{[N_2] \times [Si]}, \tag{3}$$

where $[Si] = 5 \times 10^{22}\,cm^{-3}$; i.e., the atomic density of silicon crystal, $[N_i]$ and $[N_2]$ represent the concentrations of $N_i$ atoms and $N_2$ pairs,

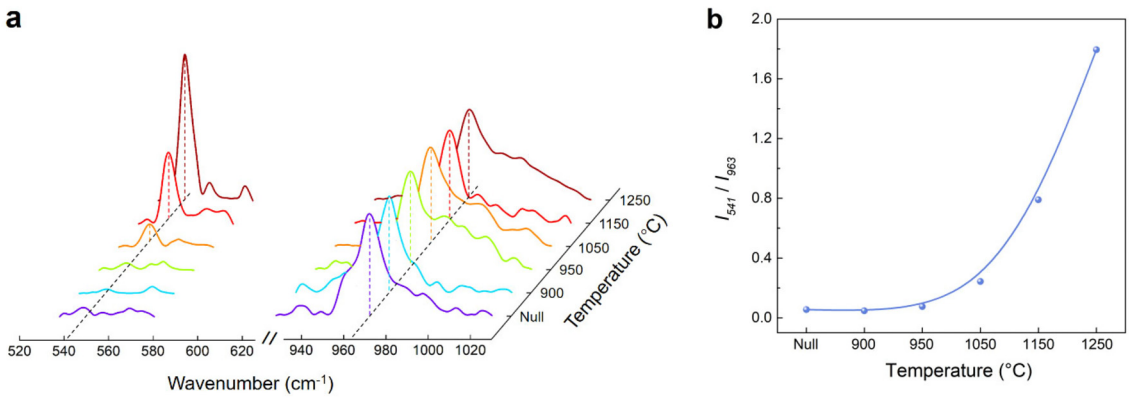


**FIG. 2.** (a) The middle-infrared FTIR spectra for the NCZ silicon specimens quenched from the isothermal anneals at different temperatures ranging from 900 to 1250 °C for 5 min, together with a reference spectrum of the as-received specimen. (b) The ratio of 541 $cm^{-1}$ peak intensity ($I_{541}$) to 963 $cm^{-1}$ peak intensity ($I_{963}$) for each specimen in (a). Herein, "Null" refers to the as-received status.

respectively. It should be mentioned that at the temperatures of 900 °C and above, the N-O complexes in different forms including the N-O STDs are substantially eliminated.[38,39] Therefore, the nitrogen impurities in the NCZ silicon specimens quenched from the isothermal anneals at the temperatures of 900 °C and above can be believed to exist predominantly in the two forms of $N_2$ pairs and $N_i$ atoms. Then, the total concentration of the nitrogen impurities ([N]) in NCZ silicon can be expressed as

$$[N] = [N_i] + 2 \times [N_2]. \tag{4}$$

Combining Eq. (3) with Eq. (4), we have

$$[N_i] = \frac{k \times [Si]}{4} \times \left( \sqrt{1 + \frac{8 \times [N]}{k \times [Si]}} - 1 \right), \tag{5}$$

$$[N_2] = \frac{[N]}{2} - \frac{k \times [Si]}{8} \times \left( \sqrt{1 + \frac{8 \times [N]}{k \times [Si]}} - 1 \right). \tag{6}$$

Understandably, the equilibrium constant $k$ is dependent on the annealing temperature. Based on the DFT calculations, the binding energy of $N_2$ pair is derived to be 3.40 eV, which is similar to those previously reported,[15,40] signifying that the dissociation of $N_2$ pairs into $N_i$ atoms is an endothermic process. Thus, the value of $k$ increases monotonically with the annealing temperature. Figure 3 shows the dependences of $[N_i]$ and $[N_2]$ on the value of $k$. Herein, the [N] is set to be $2.5 \times 10^{15}$ cm$^{-3}$, equivalent to that of the NCZ silicon wafer used in this work. Overall, the $[N_i]$ increases, while the $[N_2]$ decreases as the value of $k$ increases. In detail, when $k$ is relatively small (e.g., $<10^{-8}$) at low temperatures, $[N_2]$ is much higher than $[N_i]$. In contrast, when $k$ is relatively large (e.g., $>5 \times 10^{-8}$) at high temperatures, $[N_i]$ is much higher than $[N_2]$. The aforementioned results are indeed consistent with Fig. 2(b).

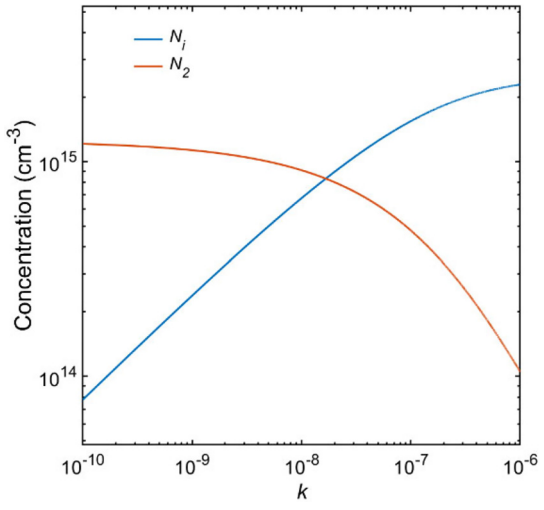


**FIG. 3.** The concentrations of $N_i$ atoms and $N_2$ pairs as a function of the equilibrium constant $k$ of the dissociation reaction from the $N_2$ pairs to the $N_i$ atoms. Herein, $k$ increases with the increasing temperature.

Figure 4(a) shows the optimized structure of a silicon supercell containing 216 Si atoms and an individual $N_2$ pair at 0 K, which is derived from the DFT calculations. The configuration of the $N_2$ pair is illustrated in the lower panel of Fig. 4(a), which is identical to that proposed by Jones *et al.*[13] Figures 4(b)–4(f) show the MD simulated atomic configurations for the silicon supercell shown in Fig. 4(a), subjected to the anneals at 900, 1050, 1150, 1200, and 1350 °C for 1 ps, respectively. Moreover, the arrangement of the Si and N atoms in each annealed supercell is also illustrated in the corresponding lower panel. Compared with the supercell at 0 K, the supercells subjected to the MD simulations at different temperatures are distorted to a large extent due to the thermal vibrations. Noteworthily, the configuration of the $N_2$ pair remains stable during the simulation at 900 or 1050 °C, indicating that the $N_2$ pair persists at these two temperatures. However, at 1150, 1200, or 1350 °C, the $N_2$ pair is no longer maintained, and it is dissociated into two $N_i$ atoms. Therefore, the MD simulations indicate that the $N_2$ pairs tend to dissociate into the $N_i$ atoms at elevated temperatures, providing a theoretical understanding for the temperature-dependent conversion between the $N_2$ pairs and $N_i$ atoms in NCZ silicon. It should be mentioned that although the $N_2$ pairs persist during the MD simulations at 900 and 1050 °C for 1 ps, the dissociation of $N_2$ pairs into the $N_i$ atoms can actually occur to some extent during the isothermal anneals at such temperatures and even lower ones, only that the equilibrium constant of the dissociation reaction is considerably small.

As an extension of significance, the evolution of nitrogen impurities themselves during the crystal growth of NCZ silicon is worthy to be addressed on the basis of the results achieved in this work. Herein, for the sake of simplicity, the interactions among the nitrogen impurities, point defects, and oxygen impurities are not considered tentatively. In the molten silicon, the doped nitrogen impurities exist overwhelmingly as the individual nitrogen atoms. As the silicon solidifies through the solid–melt interface, the individual nitrogen atoms are incorporated into the silicon crystal, turning into the $N_i$ atoms in the crystal lattice of silicon. Along with the cooling of the grown silicon crystal, the $N_i$ atoms are constantly converted into the $N_2$ pairs. As the silicon crystal is cooled below ~1050 °C, the $N_2$ pairs become the predominant species of the doped nitrogen impurities. Consequently, in the as-received NCZ silicon crystal, the doped nitrogen impurities exist predominantly as the $N_2$ pairs, which can be manifested by the 963 cm$^{-1}$ absorption peak in the FTIR spectrum in the case of sufficiently high nitrogen-doping concentration.

In summary, this work has provided a comprehensive insight into the evolution of nitrogen impurities in CZ silicon at various temperatures. Above all, by means of a dedicated quenching from the high temperature anneal of NCZ silicon, our experiment has proved the existence of $N_i$ atoms in silicon, which was only predicted by the logic derivations and theoretical calculations previously. In addition, the conversions between the $N_2$ pairs and $N_i$ atoms in the NCZ silicon quenched from different elevated temperatures are clearly demonstrated. It is found that the $[N_i]$ increases while the $[N_2]$ decreases with increasing temperature, which can be understood from a thermodynamic perspective. The MD simulations indicate that the $N_2$ pairs are indeed dissociated into the $N_i$ atoms at the temperatures of 1150 °C and above, in agreement with the experimental results. In a word, the nitrogen impurities predominantly exist as the $N_i$ atoms at high temperatures and as the $N_2$ pairs at low temperatures. Such a finding

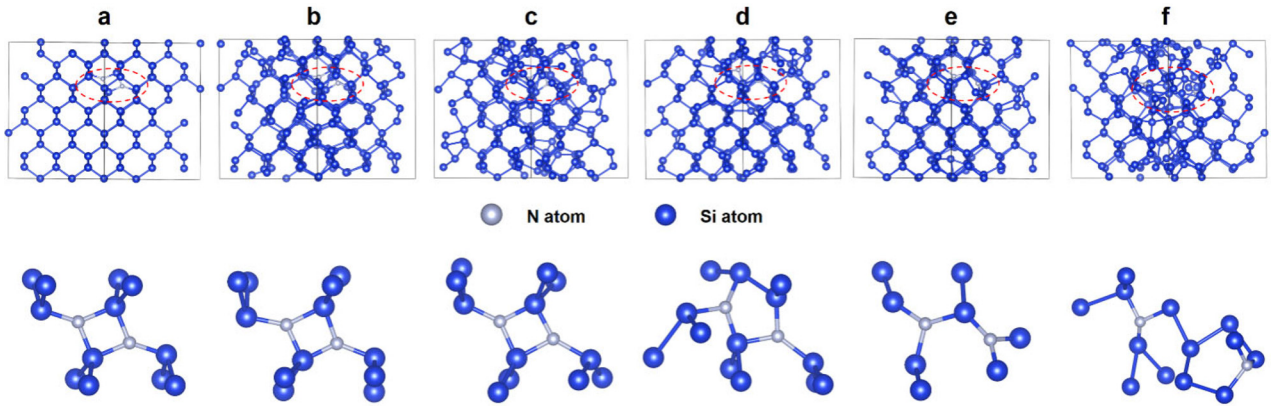


**FIG. 4.** (a) The optimized structure of a silicon supercell containing 216 Si atoms and an individual $N_2$ pair at 0 K. The configuration of $N_2$ pair is displayed in the lower panel. (b)–(f) The MD simulated atomic configuration for the silicon supercell shown in (a), subjected to the anneal at: 900 °C (b), 1050 °C (c), 1150 °C (d), 1200 °C (e), and 1350 °C (f) for 1 ps. The arrangement of Si and N atoms in each annealed supercell is illustrated in the corresponding lower panel.

represents a standpoint to understand how the nitrogen impurities evolve starting from the silicon melt to the grown silicon crystal. Moreover, the mechanism underlying the defect engineering via nitrogen-doping can be further explored based on the achievements of this work.

This work was supported by the Natural Science Foundation of China (Grant No. 62174145).

## AUTHOR DECLARATIONS

### Conflict of Interest

The authors have no conflicts to disclose.

### Author Contributions

Tong Zhao and Defan Wu equally contributed to this work.

**Tong Zhao:** Data curation (lead); Formal analysis (equal); Methodology (lead); Visualization (lead); Writing – original draft (equal). **Defan Wu:** Data curation (lead); Formal analysis (equal); Methodology (lead); Visualization (equal); Writing – original draft (equal). **Qunlin Nie:** Data curation (supporting); Validation (equal). **Hao Chen:** Data curation (supporting); Validation (equal). **Xiangyang Ma:** Conceptualization (lead); Resources (lead); Supervision (lead); Writing – review & editing (lead). **Deren Yang:** Resources (lead); Supervision (lead).

## DATA AVAILABILITY

The data that support the findings of this study are available from the corresponding authors upon reasonable request.

## REFERENCES

[1]K. Sumino, I. Yonenaga, M. Imai, and T. Abe, J. Appl. Phys. **54**, 5016–5020 (1983).
[2]J. Murphy, C. Alpass, A. Giannattasio, S. Senkader, R. Falster, and P. Wilshaw, Nucl. Instrum. Methods Phys. Res., Sect. B **253**, 113–117 (2006).
[3]X. Yu, D. Yang, X. Ma, J. Yang, L. Li, and D. Que, J. Appl. Phys. **92**, 188–194 (2002).
[4]A. Karoui, F. S. Karoui, G. A. Rozgonyi, and D. Yang, J. Appl. Phys. **96**, 3255–3263 (2004).
[5]A. Karoui and G. A. Rozgonyi, J. Appl. Phys. **96**, 3264–3271 (2004).
[6]K. Nakai, Y. Inoue, H. Yokota, A. Ikari, J. Takahashi, A. Tachikawa, K. Kitahara, Y. Ohta, and W. Ohashi, J. Appl. Phys. **89**, 4301–4309 (2001).
[7]F. Shimura and R. S. Hockett, Appl. Phys. Lett. **48**, 224–226 (1986).
[8]Q. Sun, K. H. Yao, H. C. Gatos, and J. Lagowski, J. Appl. Phys. **71**, 3760–3765 (1992).
[9]K. Aihara, H. Takeno, Y. Hayamizu, M. Tamatsuka, and T. Masui, J. Appl. Phys. **88**, 3705–3707 (2000).
[10]G. Kissinger, T. Müller, A. Sattler, W. Häckl, M. Weber, U. Lambert, A. Huber, P. Krottenthaler, H. Richter, and W. von Ammon, Solid State Phenom. **108–109**, 17–24 (2005).
[11]G. Kissinger, U. Lambert, M. Weber, F. Bittersberger, T. Müller, H. Richter, and W. von Ammon, Phys. Status Solid A **203**, 677–684 (2006).
[12]M. Qi, S. Tan, B. Zhu, P. Cai, W. Gu, X. Xu, T. Shi, D. Que, and L. Li, J. Appl. Phys. **69**, 3775–3777 (1991).
[13]R. Jones, S. Öberg, F. Berg Rasmussen, and B. Bech Nielsen, Phys. Rev. Lett. **72**, 1882–1885 (1994).
[14]R. Jones, C. Ewels, J. Goss, L. Miro, P. Deák, S. Öberg, and F. Berg Rasmussen, Semicond. Sci. Technol. **9**, 2145–2148 (1994).
[15]H. Sawada and K. Kawakami, Phys. Rev. B **62**, 1851–1858 (2000).
[16]E. Sgourou, N. Sarlis, A. Chroneos, and C. Londos, Appl. Sci. **14**, 1631 (2024).
[17]A. Hara, T. Fukuda, T. Miyabo, and I. Hirai, Appl. Phys. Lett. **54**, 626–628 (1989).
[18]C. Hu, Y. Huang, H. Ye, S. Shen, and M. Qi, Appl. Phys. Lett. **59**, 2260–2262 (1991).
[19]C. Chen, C. Li, H. Ye, S. Shen, and D. Yang, J. Appl. Phys. **76**, 3347–3350 (1994).
[20]D. Yang, R. Fan, L. Li, D. Que, and K. Sumino, Appl. Phys. Lett. **68**, 487–489 (1996).
[21]R. Newman, J. Tucker, N. Semaltianos, E. Lightowlers, T. Gregorkiewicz, I. Zevenbergen, and C. Ammerlaan, Phys. Rev.B **54**, R6803–R6806 (1996).
[22]H. Alt and H. Wagner, Phys. Rev. B **82**, 115203 (2010).
[23]T. Zhao, D. Wu, W. Lan, D. Yang, and X. Ma, J. Appl. Phys. **131**, 155703 (2022).
[24]V. Voronkov, M. Porrini, P. Collareta, M. Pretto, R. Scala, R. Falster, G. Voronkova, A. Batunina, V. Golovina, L. Arapkina, A. Guliaeva, and M. Milvidski, J. Appl. Phys. **89**, 4289–4293 (2001).
[25]L. Adam, M. Law, K. Jones, O. Dokumaci, C. Murthy, and S. Hegde, J. Appl. Phys. **87**, 2282–2284 (2000).
[26]P. Schultz and J. Nelson, Appl. Phys. Lett. **78**, 736–738 (2001).
[27]L. Adam, M. Law, O. Dokumaci, and S. Hegde, J. Appl. Phys. **91**, 1894–1900 (2002).

[28]V. Voronkov, A. Batunina, G. Voronkova, and M. Mil'vidskiĭ, Phys. Solid State **46**, 1206–1212 (2004).
[29]C. Alpass, J. Murphy, R. Falster, and P. Wilshaw, J. Appl. Phys. **105**, 013519 (2009).
[30]T. Itoh and T. Abe, Appl. Phys. Lett. **53**, 39–41 (1988).
[31]H. Sawada, K. Kawakami, A. Ikari, and W. Ohashi, Phys. Rev. B **65**, 075201 (2002).
[32]K. Tanahashi, H. Yamada-Kaneta, and N. Inoue, Jpn. J. Appl. Phys., Part 2 **43**, L436–L438 (2004).
[33]N. Fujita, R. Jones, J. Goss, P. Briddon, T. Frauenheim, and S. Öberg, Appl. Phys. Lett. **87**, 021902 (2005).
[34]N. Stoddard, P. Pichler, G. Duscher, and W. Windl, Phys. Rev. Lett. **95**, 025901 (2005).
[35]J. Goss, I. Hahn, R. Jones, P. Briddon, and S. Öberg, Phys. Rev. B **67**, 045206 (2003).
[36]J. Perdew, K. Burke, and M. Ernzerhof, Phys. Rev. Lett. **77**, 3865–3868 (1996).
[37]J. Perdew, K. Burke, and Y. Wang, Phys. Rev. B **54**, 16533–16539 (1996).
[38]J. Libbert, L. Mule'Stagno, and M. Banan, J. Appl. Phys. **92**, 1238–1241 (2002).
[39]T. Zhao, C. Hua, W. Lan, Y. Sun, D. Wu, Y. Lu, X. Ma, and D. Yang, J. Appl. Phys. **129**, 145702 (2021).
[40]H. Kageshima, A. Taguchi, and K. Wada, Appl. Phys. Lett. **76**, 3718–3720 (2000).